Supporting Information

Label-free electrochemical aptasensor based on the core-shell Cu-MOF@TpBD hybrid nanoarchitecture for the sensitive detection of PDGF-BB

Ya Li,[a] Zhiling Liu,[a] Wenbo Lu,[a] Man Zhao,[a] He Xiao,[a] Tianjun Hu,[a] Jianchun Ma,[a] Zhanfeng Zheng,[b] Jianfeng Jia*[a] and Haishun Wu*[a]

[a]Key Laboratory of Magnetic Molecules and Magnetic Information Materials Ministry of Education, School of Chemical and Material Science, Shanxi Normal University, Linfen 041004, China

[b]State Key Laboratory of Coal Conversion, Institute of Coal Chemistry, Chinese Academy of Sciences

Corresponding authors

*E-mail: jiajf@dns.sxnu.edu.cn

*E-mail: wuhs@sxnu.edu.cn

S1. Experimental section

S1.1. Reagents and Materials

1, 3, 5-triformylphloroglucinol (Tp) and mesitylene and benzidine (BD) were purchased from Energy Chemical (Shanghai, China). Copper (II) nitrate trihydrate ($Cu(NO_3)_2 \cdot 3H_2O$) and acetic acid and dichloromethane (DCM) were purchased from Hushi Laboratorial Equipment Co. Ltd. (Shanghai, China). Gold chloride tetrahydrate ($HAuCl_4 \cdot 4H_2O$, 99.9%), acetone, and 1,4-dioxane were purchased from Sinopharm Chemical Reagent Co.Ltd. (Shanghai, China). Human mucin1 (MUC1) vascular endothelial growth factor (VEGF) and (platelet-derived growth factor-BB) PDGF-BB were purchased from Shanghai North Connaught Biotechnology Co, Ltd. (Shanghai, China). Human serum was provided by Linfen People's Hospital (Shanxi, China). 2-amino terephthalic acid (NH_2-BDC) was provided by Bailingwei Chemical Technology Co. Ltd. (Beijing, China). N, N-dimethylformamide (DMF, ≥ 99%) was provided by Aladdin (China). Polyvinylpyrrolidone (PVP, Mw = 40000 $g \cdot mol^{-1}$) was obtained from Stremchemical. Phosphate buffer solution (PBS, 0.1 M, pH 7.4) containing 0.1 M Na_2HPO_4, 0.1 M KH_2PO_4, and 0.1 M KCl was used as a working buffer for the performance examination of the electrodes. The ultra-pure water was used throughout the whole experiment. The sequences of PDGF-BB targeted aptamer is listed as follows: CAGGCTACGGCACGTAGAGCATCACCATGATCCTG.

S1.2. Apparatus

Valuable information about the topographic characteristics of the synthetic nanomaterials was captured with the aid of JEOL JSM-7500F field emission scanning electron microscope (SEM) and JEOL JEM-2100 transmission electron microscope (TEM). The phase structure of the nanomaterials was analyzed using the Rigaku Ultima IV-185 room-temperature X-ray diffractometer (XRD) with filtered Cu Kα radiation. The comparative Fourier transformation infrared spectra (FTIR) were recorded with a Bruker Alpha FTIR spectrometer. The specific surface areas

and pore size distribution of all samples were measured by the method of Brunauer-Emmett-Teller (BET) using a Beishide 3H-2000PS2 instrument at the temperature of liquid nitrogen.

S1.3. Electrochemical detection

The whole electrochemical measurements were conducted at room temperature with a CHI660E electrochemical workstation (Chenhua Instrument Company of Shanghai, China), which equips with a conventional three-electrode configuration consisting of a glassy carbon electrode (GCE, 4 mm in diameter), a saturated calomel electrode (SCE), and a platinum wire. The mixed solution comprising $K_3[Fe(CN)_6]/K_4[Fe(CN)_6]$ (5 mM) and KCl (0.1 M) was utilized as the electrolyte solution for the cyclic voltammetry (CV) measurement. The sweeping rate of the CV measurements was 50 $mV \cdot s^{-1}$, which were carried out in the range between -0.2 and 0.6 V (*vs.* SCE). The target of PDGF-BB was examined by the differential pulse voltammetry (DPV) measurements, which were performed in the potential of -0.2–0.3 V (*vs.* SCE) with an amplitude of 50 mV and a pulse width of 0.05 s.

S1.4. Theoretical calculations

To qualitatively understand the weak interactions between the TpBD and aptamer, the model of TpBD-aptamer complex was set up and then further theoretically optimized with xTB program.[1, 2] The obtained molden file was used for the wavefunction analyses, which were finished by using Multiwfn program.[3] The Independent Gradient Model (IGM)[4] was employed for the visually studying inter-fragment interactions between TpBD and truncated PDGF-BB targeted aptamer. The color-coded isosurface images of IGM were rendered and visualized by the VMD program.[5]

References

1. S. Grimme, C. Bannwarth and P. Shushkov, A Robust and Accurate Tight-Binding Quantum Chemical Method for Structures, Vibrational Frequencies, and Noncovalent Interactions of Large Molecular Systems Parametrized for All spd-Block Elements (Z = 1–86), *J. Chem. Theory*

Comput., 2017, **13**, 1989.

2. C. Bannwarth, S. Ehlert and S. Grimme, GFN2-xTB—An Accurate and Broadly Parametrized Self-Consistent Tight-Binding Quantum Chemical Method with Multipole Electrostatics and Density-Dependent Dispersion Contributions, *J. Chem. Theory Comput.*, 2019, **15**, 1652.

3. T. Lu and F. W. Chen, Multiwfn: A Multifunctional Wavefunction Analyzer, *J. Comput. Chem.*, 2012, **33**, 580.

4. C. Lefebvre, G. Rubez, H. Khartabil, J.-C. Boisson, J. Contreras-García and E. Hénon, Accurately Extracting the Signature of Intermolecular Interactions Present in the NCI Plot of the Reduced Density Gradient versus Electron Density, *Phys. Chem. Chem. Phys.*, 2017, **19**, 17928.

5. W. Humphrey, A. Dalke and K. Schulten, VMD: Visual Molecular Dynamics, *J. Mol. Graphics.*, 1996, **14**, 33.

Table S1 Comparison of different approaches in analyzing PDGF-BB.

Method	Detection range	Detection limit	Source
Electrochemical impedance spectroscopy	0.001−0.05 ng·mL^{-1}	0.82 pg·mL^{-1}	ref. 6
Electrochemical impedance spectroscopy	0.01−100 ng·mL^{-1}	3.7 pg·mL^{-1}	ref. 7
Differential pulse voltammetry	0.005−1000 ng·mL^{-1}	1.6 pg·mL^{-1}	ref. 8
Biolayer interferometry	0.5−1000 ng·mL^{-1}	80 pg·mL^{-1}	ref. 9
ELISA	0.00206−1.5 ng·mL^{-1}	2.1 pg·mL^{-1}	abcam
Differential pulse voltammetry	0.0001−0.5 and 0.5−60 ng·mL^{-1}	0.034 pg·mL^{-1}	This work

6. Z. Zhang, C. Guo, S. Zhang, L. He, M. Wang, D. Peng, J. Tian and S. Fang, Carbon-based nanocomposites with aptamer-templated silver nanoclusters for the highly sensitive and selective detection of platelet-derived growth factor, *Biosens. Bioelectron.*, 2017, **89**, 735.

7. L. He, S. Zhang, H. Ji, M. Wang, D. Peng, F. Yan, S. Fang, H. Zhang, C. Jia and Z. Zhang,

Protein-templated cobaltous phosphate nanocomposites for the highly sensitive and selective detection of platelet-derived growth factor-BB, *Biosens. Bioelectron.*, 2016, **79**, 553.

8. W. Song, H. Li, H. Liang, W. Qiang and D. Xu, Disposable Electrochemical Aptasensor Array by Using in Situ DNA Hybridization Inducing Silver Nanoparticles Aggregate for Signal Amplification, *Anal. Chem.*, 2014, **86**, 2775.

9. S. Gao, X. Zheng and J. Wu, A biolayer interferometry-based enzyme-linked aptamer sorbent assay for real-time and highly sensitive detection of PDGF-BB, *Biosens. Bioelectron.*, 2018, **102**, 57.

Table S2 Detection of PDGF-BB added in human serum (n = 6).

Samples	Added PDGF-BB ($ng \cdot mL^{-1}$)	Found PDGF-BB ($ng \cdot mL^{-1}$)	Recovery (%)	RSD (%)
1	0.0001	0.000091	91.0	4.3
2	0.5	0.487	97.4	3.8
3	5	5.395	107.9	2.9
4	20	18.62	93.1	3.7
5	40	39.35	98.4	4.5

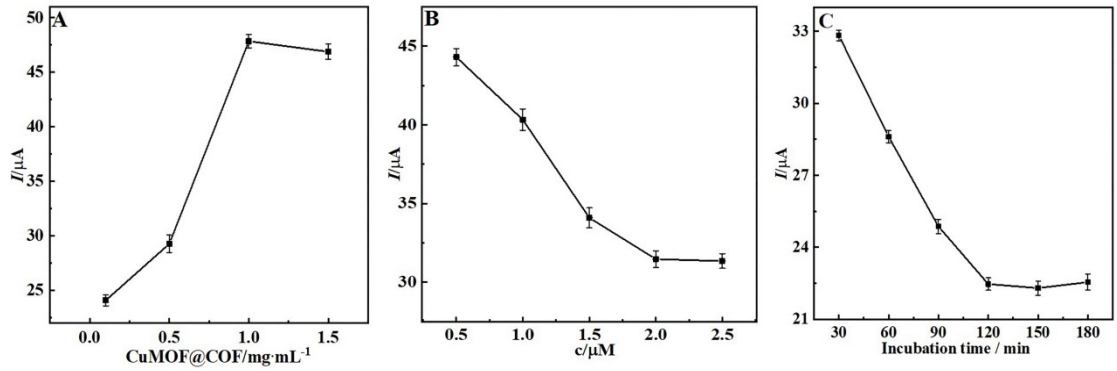

Fig. S1 The current responses of (A) DpAu/GCE electrode incubated with different concentrations Cu-MOF@TpBD, (B) Cu-MOF@TpBD/DpAu/GCE electrode incubated with different concentration of aptamers. (C) the amperometric response of aptasensor as the function of the incubation time when immune-reacted with 500 pg·mL^{-1} PDGF-BB. The standard deviations of the mean are indicated as error bars, with the determination of 4 (n = 4).

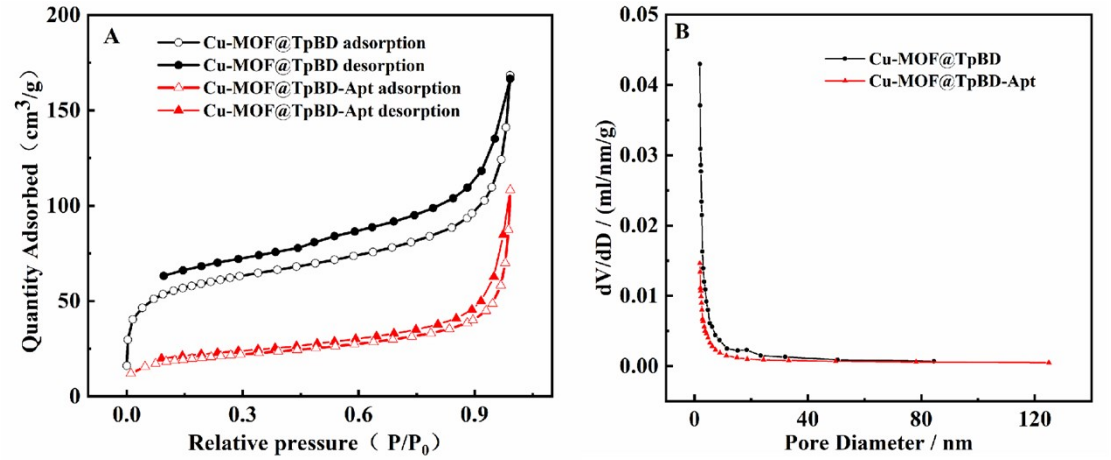

Fig. S2 N_2 adsorption-desorption isotherms (A) and the corresponding pore-size distribution curves (B) of the samples Cu-MOF@TpBD and Cu-MOF@TpBD-Apt.